A NUMERICALLY BASED INVESTIGATION ON THE SYMMETRY BREAKING AND ASYMPTOTIC BEHAVIOR OF THE GROUND STATES TO THE p-HÉNON EQUATION

XUDONG YAO, JIANXIN ZHOU

ABSTRACT. The symmetry breaking phenomenon (SBP) to the Hénon equation was first numerically observed in [4] and then theoretically verified on the unit ball B_n in [8]. Some results on the asymptotic behavior of the ground states to the Hénon equation on B_n are presented in [2, 3, 7]. [8] further discussed SBP to the p-Hénon equation and obtained some results with special value $p \leq n$ on B_n. To inspire theoretical study on more general p, a series of numerical experiments to the p-Hénon equation on a disk and a square are carried out in this paper. Numerical computations are made by the minimax method developed in [9, 10]. Then, SBP, a peak break phenomenon (PBP); i.e., a 1-peak solution, which is symmetric about two axes and two diagonal lines, breaks its peak from 1 to 4, and a 1-peak positive non-ground state solution, which is only symmetric about one axis, on the square are numerically captured and visualized. The peak point and the peak height of the ground states are carefully calculated to study their asymptotic behavior. Several conjectures are made based on the numerical observations to stimulate theoretical analysis. Two of them are proved in this paper.

1. INTRODUCTION

Consider the p-Hénon equation, a quasi-linear elliptic boundary value problem (BVP) of the form

$$\Delta_p u + |x|^r |u|^{q-2} u = 0, \quad x \in \Omega, \ u \in W_0^{1,p}(\Omega), \tag{1.1}$$

where Δ_p is the p-Laplacian operator defined by $\Delta_p u = \operatorname{div}(|\nabla u|^{p-2}\nabla u)$ $(p > 1)$, $\Omega \subset \mathbb{R}^n$ is a bounded open domain, $|x|$ is the Euclidian norm of x, $p < q < p^*$ (p^* is the Sobolev exponent) and $r \geq 0$. The original Hénon equation $(p = 2)$ was proposed by French astronomer and mathematician Michel Hénon [6] to improve a model by the Lane-Emden (-Fowler) equation $(p = 2, r = 0)$ in astrophysics in study of stellar systems. The study of the Hénon equation has crossed several disciplinary branches. Many interesting properties, such as solution multiplicity and various structures, bifurcation, chaos, ..., are explored. This equation was modified in several different ways and becomes an important model in the study of nonlinear

dynamic systems. One of the important modifications leads to the p-Hénon equation due to applications in physical fields, typically in non-Newtonian/Darcian fluid flows or materials, where the shear stress $\vec{\tau}$ and the velocity gradient ∇u of the fluid are related in the manner $\vec{\tau}(x) = r(x)|\nabla u|^{p-2}\nabla u$. When $p = 2$, $\Delta_p = \Delta$ is the Laplacian operator whose wide applications are well-known and typical in the study of Newtonian/Darcian fluid/material. When $p \neq 2$, the p-Laplacian operator has a variety of applications in physical fields and theoretical study as well, such as in the study of Non-Newtonian/Darcian fluid/material. For example, the fluid/material is called pseudo plastic if $p < 2$ and dilatant if $p > 2$. The p-Laplacian operator also appears in the study of flow in a porous media ($p = 3/2$), nonlinear elasticity ($p > 2$) and glaciology ($p \in (1, 4/3)$) [5].

It is quite natural for researchers to carry out parallel study of the p-Hénon equation to the path of successful study of the Hénon equation. Since $u = 0$ is always a trivial solution to (1.1), people are interested in knowing the existence or non-existence of nontrivial solutions, the number of solutions as well as their structures in terms of qualitative properties such as the geometric, symmetric and nodal (peak) properties in different energy levels.

Mathematically it is known that the Hénon and the p-Hénon equation belong to two classes of partial differential equations with different complexities. The former is of semilinear elliptic BVP since its derivative term is linear and can be handled in a Hilbert space setting. While the later is of quasilinear elliptic BVP since its derivative term is nonlinear. It has to be handled in a Banach space setting and thus much tougher to analysis. Consequently the regularity of solutions to the p-Hénon equation is weaker. Due to its Banach space setting, even numerically the p-Hénon equation is much more difficult to solve, see [9, 10, 11].

Though great progress has been made still many important open questions remain unsettled. For instance, as one of many significant differences between Δ and Δ_p, the authors numerically showed in [11] that on a square the second eigenvalue of $-\Delta_p$ splits from a double eigenvalue into two simple eigenvalues when p moves from 2 to $\neq 2$. Such an interesting difference has not yet been theoretically verified.

Symmetry is one of the important characteristics to understand solution structures. When $p = 2$ and $r = 0$, the well-known Gidas-Ni-Nirenberg [1] theorem states that if Ω is the unit ball in $\mathbb{R}^n$, then it implies that the positive ground state of (1.1) is radial. When $p = 2$ and $r > 0$, the equation (1.1) has an explicit dependence on x. Although radial symmetry is still kept to (1.1), the Gidas-Ni-Nirenberg theorem cannot be applied and the radial positive solution may give up its ground state to new radially asymmetric positive solutions. Such a phenomenon is called a *symmetry breaking phenomenon* (SBP) and was first numerically observed in [4]. It immediately draws attentions. Several researchers have theoretically verified the existence of such phenomenon [8] and obtained results on asymptotic behavior of the ground states [2, 3, 7] when $r \to \infty$ and p, q are fixed. Researchers have also tried to study SBP for the p-Hénon equation (1.1) ($p \neq 2$) on the unit ball $\Omega = B_n$ in $\mathbb{R}^n$. But results are very limited to the value of p. For example, Theorem 8.2 in [8] shows that if $n > p$ and $n \geq 2$, then, for any $p < q < p^*$, SBP must occur when r exceeds certain number; in [2, 3, 7], when $p = 2$, q is fixed and $r \to \infty$, asymptotic behavior of the ground states of (1.1) is discussed. As the results in the literature are under the assumption $p = 2$ or $p < n$, it is quite natural to ask if SBP to (1.1)

will take place when $p \neq 2$, in particular, when $n \leq p$ ($p > 2$ corresponds to dilatant fluid/material) and to study asymptotic behavior of the ground states when $p \neq 2$. So far no theoretical answer is available. When $p = 2$, $r = 0$ and Ω is a non-radial domain, the Berestycki-Nirenberg theorem [1], a beautiful generalization of the Gidas-Ni-Nirenberg theorem, says that if Ω is symmetric about a hyperplane in $\mathbb{R}^n$, then the positive ground state of (1.1) is also symmetric about the hyperplane. Similar to the Gidas-Ni-Nirenberg theorem, the Berestycki-Nirenberg theorem does not work to (1.1) with $r > 0$, although, to (1.1), symmetry about any hyperplane passing through the origin is still there. In other words, the positive ground states may be asymmetric about a hyperplane passing through the origin although the domain Ω is symmetric about it. This phenomenon is also called SBP. On symmetry of the positive ground states of (1.1) with $r > 0$ on a non-radial domain Ω, *little research is done*. As the first step, we would like to investigate (1.1) on simple non-radial domains which are symmetric about some hyperplanes passing through the origin to see if the positive ground states have same symmetry or not. Among these domains, the hypercubic domains $(-a, a)^n$, $a > 0$, are good candidates. They have simple structure and symmetry about every coordinate hyperplane. Due to the form of (1.1), if u_1 is a solution on $(-a_1, a_1)^n$, $a_1 > 0$, then $u_2(x) = ku_1(\frac{a_1}{a_2}x)$ is a solution on $(-a_2, a_2)^n$, $a_2 > 0$, where $k = (\frac{a_1}{a_2})^{\frac{p+r}{q-p}}$. Hence, the value of a has no influence on symmetry. Similarly, the value of radius has no influence on radial symmetry in the study of solutions to (1.1) on a ball of center at the origin. In Theorem 2.1 and Theorem 2.4, we will draw conclusions on general domains about asymptotic behavior of the positive ground states to (1.1) by observing numerical results on B_2 and $(-1,1)^2$. So, in this paper, the minimax method developed by the authors in [9, 10] is applied to carry out a series of numerical investigations of the p-Hénon equation on *the disk B_2* and *the square $(-1,1)^2$* about SBP and asymptotic behavior of its positive ground states. Through numerical computation and visualization, we try to figure out a possible answer to stimulate further theoretical study.

The corresponding energy functional of (1.1) is

$$J(u) = \int_\Omega \Big[\frac{1}{p}|\nabla u(x)|^p - \frac{1}{q}|x|^r|u(x)|^q\Big]dx, \quad \forall u \in W_0^{1,p}(\Omega). \qquad (1.2)$$

Then, for each $v \in W_0^{1,p}(\Omega)$,

$$\begin{aligned}
\langle \nabla J(u), v\rangle &= \frac{d}{ds}J(u+sv)\Big|_{s=0} \\
&= \int_\Omega \Big[|\nabla u(x)|^{p-2}\nabla u(x) \cdot \nabla v(x) - |x|^r|u(x)|^{q-2}u(x)v(x)\Big]dx \\
&= \int_\Omega \Big[-\nabla(|\nabla u(x)|^{p-2}\nabla u(x))v(x) - |x|^r|u(x)|^{q-2}u(x)v(x)\Big]dx \\
&= \int_\Omega \Big[-\Delta_p u(x) - |x|^r|u(x)|^{q-2}u(x)\Big]v(x)dx.
\end{aligned}$$

Thus it is clear that weak solutions of (1.1) coincide with critical points of J, i.e., $\nabla J(u) = 0$. The first candidates of critical points are the local extrema. Traditional calculus of variation and numerical methods focus on finding such stable solutions. As for J in (1.2), the only local extremum is the local minimum, the trivial solution $u \equiv 0$. Critical points that are not local extrema are unstable and

called saddle points. Numerically computing those saddle points in a stable way
is very challenging due to their instability and multiplicity. A numerical minimax
method is developed by the authors in [9] for finding multiple saddle points in a
Banach space following a sequential order. Its convergence is established in [10].
By this method, we could carry out efficient and reliable numerical experiments on
(1.1). Since for $p > 2$, the regularity of solutions to (1.1) is weaker, for possible
weak solutions u, the peak height has to be defined by the essential supremum
(ess. sup) of $|u|$ instead of maximum (max) of $|u|$ and the peak point is then defined
to be the set of all points whose any neighborhoods have the essential supremum
of $|u|$ equal to the peak height.

In our numerical experiments, the Sobolev norm $\|\nabla J(u)\| < 0.005$ is used to
terminate an iteration in our local minimax method. On both domains, SBP are
found in our numerical experiments when r is large. The peak point and peak
height of the ground state are carefully calculated, which provides us with some
information on their asymptotic behavior as the parameter $r \to +\infty$. Through
our numerical computation on a square, we captured a peak breaking phenomenon
(PBP), i.e., the 1-peak positive solution, which is symmetric about the lines $x = 0$,
$y = 0$ and $y = \pm x$, breaks its peak from one to four when r increases and exceeds a
certain value; we also numerically found 1-peak non-ground state solutions, which
is only symmetric about the line $x = 0$ or $y = 0$, by enforcing this symmetry in the
computation. Finally we make some mathematical analysis and conjectures based
on our numerical observations.

At the end of this section, we attach the flow chart of our minimax algorithm
for numerically finding multiple solutions of p-Laplacian equation in [9, 10]. In
Step 3, the descent direction is calculated by ∇J. This is a computing technique
developed by us [9, 10] for p-Laplacian equation. Assume that $u_1, u_2, \ldots, u_{n-1}$
are found critical points of $J \in C^1(W_0^{1,\bar{p}}(\Omega), \mathbb{R})$, $L = [u_1, u_2, \ldots, u_{n-1}]$, i.e., the
subspace of $W_0^{1,\bar{p}}(\Omega)$ spanned by $u_1, u_2, \ldots, u_{n-1}$, $\Omega \subset \mathbb{R}^n$ is an open, bounded set
and $\frac{1}{\bar{p}} + \frac{1}{\bar{q}} = 1$, $\bar{p}, \bar{q} > 0$. We denote $\| \cdot \|_{\bar{r}}$ as $\| \cdot \|_{W_0^{1,\bar{r}}(\Omega)}$ for $\bar{r} > 1$. $\epsilon > 0$ is a
small number and $0 < \lambda < 1$ is a constant. The following is the flow chart of the
algorithm.

Step 1: Let $v_n^1 \in S_{L^\perp}$.
Step 2: Set $k = 1$ and solve for

$$u_n^k = P(v_n^k) = t_0^k v_n^k + t_1^k u_1 + \cdots + t_{n-1}^k u_{n-1}$$
$$= \arg\max\{J(t_0 v_n^k + t_1 u_1 + \cdots + t_{n-1} u_{n-1}) | t_i \in \mathbb{R}, i = 0, 1, \ldots, n-1\}.$$

Step 3: Find a descent direction $w_n^k = -sign(t_0^k)\nabla J(u_n^k)$ at $u_n^k = P(v_n^k)$.
Step 4: If $\|\nabla J(u_n^k)\|_{\bar{q}} < \varepsilon$, then output u_n^k, stop. Otherwise, do Step 5.
Step 5: For each $s > 0$, let

$$v_n^k(s) = \frac{v_n^k + s w_n^k}{\|v_n^k + s w_n^k\|_{\bar{p}}}$$

and use the initial point $(t_0^k, t_1^k, \ldots, t_{n-1}^k)$ to solve for

$$P(v_n^k(s)) = \arg\max\left\{J(t_0 v_n^k(s) + \sum_{i=1}^{n-1} t_i u_i) | t_i \in \mathbb{R}, i = 0, 1, \ldots, n-1\right\},$$

then set $v_n^{k+1} = v_n^k(s_n^k)$ and $u_n^{k+1} = P(v_n^{k+1}) = t_0^{k+1}v_n^{k+1} + t_1^{k+1}u_1 + \cdots + t_{n-1}^{k+1}u_{n-1}$, where s_n^k satisfies

$$s_n^k = \max\{s = \frac{\lambda}{2^m} | m \in N, J(P(v_n^k(s))) - J(P(v_n^k)) \le -\frac{1}{4}|t_0^k|s\|\nabla J(u_n^k)\|_2^2\}.$$

Step 6: Update $k = k + 1$ and go to Step 3.

Remark 1.1. As $1 < \bar{p} < 2$, we assume that $u_1, u_2, \ldots, u_{n-1}$ are nice; i.e., $L \subset W_0^{1,\bar{q}}(\Omega)$ and $S_{L^\perp} = \{u \in W_0^{1,\bar{p}}(\Omega) | \langle u, u_i \rangle = 0, \ i = 1, \ldots, n-1 \ and \ \|u\|_{\bar{p}} = 1\}$ for $\bar{p} > 1$ in the algorithm.

2. Numerical and Analytic Results

2.1. **On the Unit Disk in $\mathbb{R}^2$.** Let us first consider the p-Hénon equation (1.1) on the unit ball $\Omega = B_n \subset \mathbb{R}^n$. Numerically we choose the unit disk $\Omega = B_2 \subset \mathbb{R}^2$. To maintain sufficient accuracy, over 10^5 triangle elements are used on B_2 in our numerical experiment. We will focus on computing ground states to see if SBP occurs. By our computation, we notice that the 1-peak positive radial solution always exists. The contours of these numerical radial solutions are presented in Fig. 1 and in (c) and (f) of Figs. 2-5. In the computation to capture the ground state, we always use a positive non-radial initial guess. If a numerical solution is radially symmetric, then our numerical experiment does not support SBP. Thus in (a) and (d) of Figs. 2-5, once a contour plot of the radially symmetric numerical solution is presented, it means that for the values of p, q, r, SBP does not occur. Otherwise, the contours of a non-radial numerical solution will be presented in (b) and (e) of Figs. 2-5. By Figs. 4 and 5, it can be concluded that SBP to (1.1) on the unit disk $\Omega = B_2$ will take place when r increases and exceeds a certain number r_b for $p = 2.5, 3.0$. Since $2 = n \le p = 2.5, 3.0$, it is reasonable to conjecture that SBP to (1.1) on the unit disk $\Omega = B_2$ will take place when r increases and exceed a certain number r_b for every $p > 2$. On the other hand, as we mentioned before, Theorem 8.2 in [8] shows that if $n > p$ and $n \ge 2$, then, for any $p < q < p^*$, SBP must occur when r increases and exceeds a certain number r_b. Hence, indeed we conjecture that SBP to (1.1) on the unit disk $\Omega = B_2$ will take place for every $p \ne 2$ when r increases and exceeds a certain number r_b. Generally, we would like to conjecture that SBP to (1.1) with $p \ne 2$ on the unit ball $\Omega = B_n$ in $\mathbb{R}^n$ will always occur when r increases and exceeds a certain number r_b. In Table 3, we give information on the location of r_b from our numerical experiment.

In Figures 2-5, if we compare (a) with (c) and (d) with (f), we can see that the top of the 1-peak radial solution becomes flatter as r increases. Next, we carry out more numerical experiments to investigate asymptotic behavior of the peak point and peak height to a positive ground state of (1.1) as $r \to +\infty$. To $(p, q) = (a)(1.75, 7.75)$, $(b)(1.75, 9.25)$, $(c)(2.0, 8.0)$, $(d)(2.0, 9.5)$, $(e)(2.5, 8.5)$, $(e)(2.5, 10.0)$, $(g)(3.0, 9.0)$, $(h)(3.0, 10.5)$, we list our numerical results in Tables 1 and 2. From Table 1, it is quit natural to conclude that the peak point $(\alpha(r), 0) \to (1, 0)$ as $r \to \infty$. From Table 2, we can see that the peak height $\beta(r)$ is monotonously increasing in r when p and q are fixed. Based on this numerical observation, we prove $\lim_{r \to +\infty} \beta(r) = +\infty$.
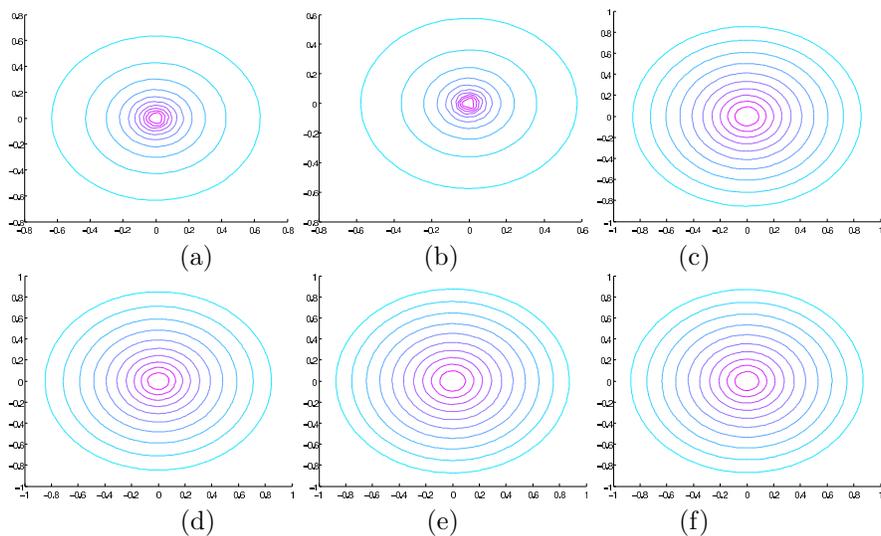
FIGURE 1. Ground states for $r = 0$: From (a) to (f) $(p, q) = (1.75, 7.75), (1.75, 9.25), (2.5, 8.5), (2.5, 10.0), (3.0, 9.0), (3.0, 10.5)$.
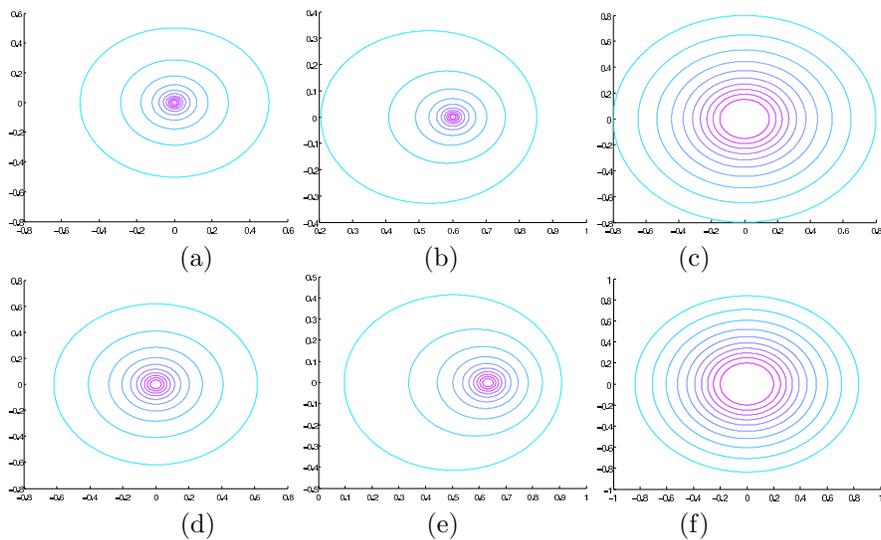

FIGURE 2. $p = 1.75$: (a) $q = 7.75$, $r = 0.001$; (b)(c) $q = 7.75$, $r = 1.4$; (d) $q = 9.25$, $r = 0.001$; (e)(f) $q = 9.25$, $r = 1.4$.
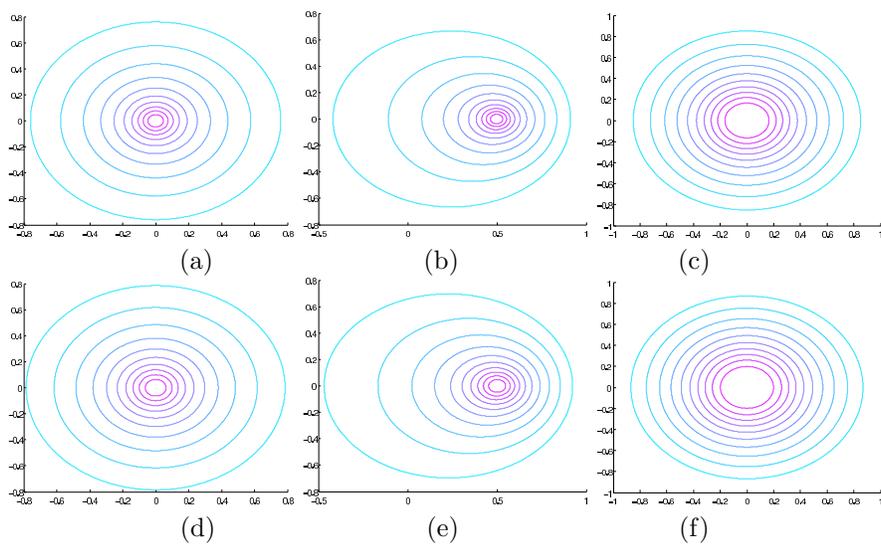
FIGURE 3. $p = 2.0$: (a) $q = 8.0$, $r = 0.001$; (b)(c) $q = 8.0$, $r = 1.4$; (d) $q = 9.5$, $r = 0.001$; (e)(f) $q = 9.5$, $r = 1.4$.
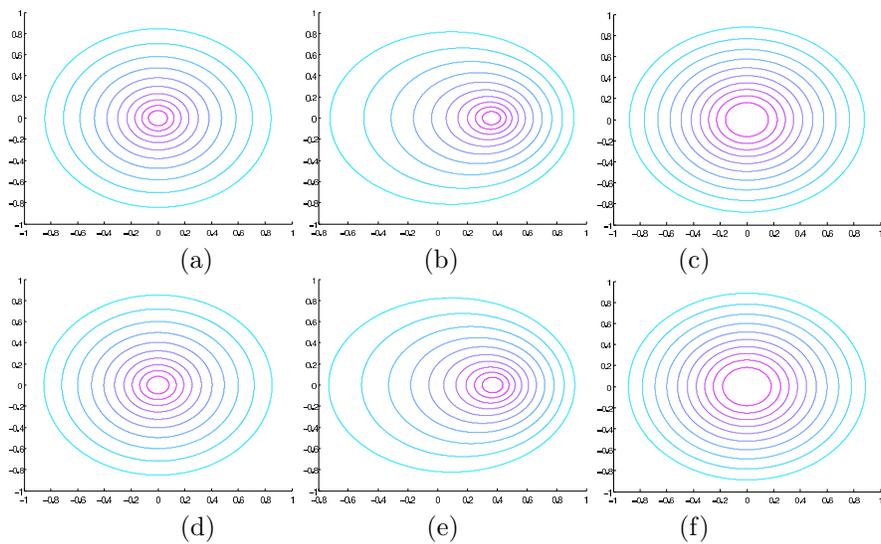

FIGURE 4. $p = 2.5$: (a) $q = 8.5$, $r = 0.001$; (b)(c) $q = 8.5$, $r = 1.4$; (d) $q = 10.0$, $r = 0.001$; (e)(f) $q = 10.0$, $r = 1.4$.
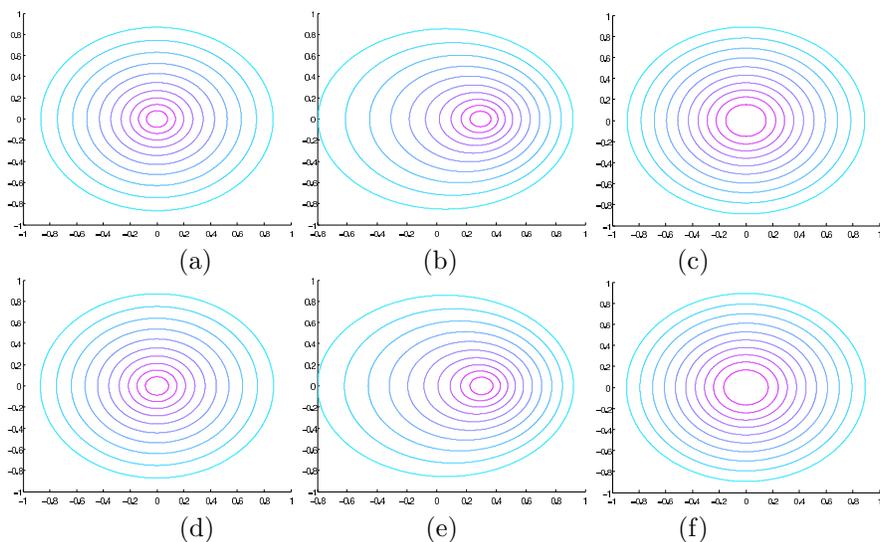
FIGURE 5. $p = 3.0$: (a) $q = 9.0$, $r = 0.001$; (b)(c) $q = 9.0$, $r = 1.4$;
(d) $q = 10.5$, $r = 0.001$; (e)(f) $q = 10.5$, $r = 1.4$.

TABLE 1. Values for α in Equation (1.1) with $(\alpha, 0)$ as peak
point of its ground state and (p, q): (a)(1.75,7.75), (b)(1.75,9.25),
(c)(2.0,8.0), (d)(2.0,9.5), (e)(2.5,8.5), (f)(2.5,10.0), (g)(3.0,9.0),
(h)(3.0,10.5)

r	(a)	(b)	(c)	(d)	(e)	(f)	(g)	(h)
1	0.5694	0.473	0.4563	0.4526	0.3238	0.3158	0.2567	0.2505
10	0.9100	0.9327	0.8475	0.8434	0.7389	0.7253	0.6673	0.6554
20	0.9469	0.9397	0.9125	0.9100	0.8382	0.8319	0.7862	0.7764
30	0.9585	0.9580	0.9366	0.9356	0.8880	0.8787	0.8444	0.8382
40	0.9667	0.9698	0.9523	0.9514	0.9097	0.9055	0.8772	0.8697
50	0.9780	0.9745	0.9605	0.9598	0.9253	0.9222	0.8974	0.8912
60	0.9812	0.9782	0.9651	0.9630	0.9356	0.9344	0.9113	0.9071
70	0.9815	0.9814	0.9682	0.9682	0.9461	0.9408	0.9249	0.9197
80	0.9846	0.9835	0.9741	0.9734	0.9503	0.9492	0.9312	0.9260
90			0.9757	0.9757	0.9576	0.9549	0.9385	0.9368
100					0.9603	0.9576	0.9447	0.9409
110							0.9489	0.9472

Table 2. Values for β in Equation (1.1) with β as peak height of its ground state and (p,q): (a)(1.75,7.75), (b)(1.75,9.25), (c)(2.0,8.0), (d)(2.0,9.5), (e)(2.5,8.5), (f)(2.5,10.0), (g)(3.0,9.0), (h)(3.0,10.5)

r	(a)	(b)	(c)	(d)	(e)	(f)	(g)	(h)
1	2.7014	2.6771	2.3321	2.1732	2.2658	2.0618	2.2963	2.0698
10	3.8074	3.6796	3.5306	3.0597	3.8002	3.1791	4.2536	3.4725
20	4.2279	4.0109	4.1718	3.5142	4.7398	3.8162	5.5682	4.3602
30	4.6128	4.2008	4.6094	3.8119	5.4016	4.2661	6.5753	4.9885
40	5.0197	4.2456	4.9304	4.0266	5.9826	4.6180	7.4031	5.5313
50	5.1745	4.4020	5.1998	4.2301	6.4534	4.9311	8.0722	5.9702
60	5.2685	4.4032	5.3939	4.3527	6.8090	5.1067	8.7009	6.3522
70	5.4229	4.5602	5.6626	4.4925	7.2276	5.3267	9.2710	6.6541
80	5.5110	4.6427	5.9859	4.5949	7.4819	5.5139	9.7939	6.9534
90			6.0895	4.6753	7.8675	5.7908	10.3577	7.3044
100					8.1275	5.9344	10.8145	7.5803
110							11.2683	7.8350

Table 3. $r_b \in (r_1, r_2)$ for (p,q): (a)(1.75,7.75), (b)(1.75,9.25), (c)(2.0,8.0), (d)(2.0,9.5), (e)(2.5,8.5), (f)(2.5,10.0), (g)(3.0,9.0), (h)(3.0,10.5)

	(a)	(b)	(c)	(d)
(r_1, r_2)	(0.0027,0.0054)	(0.0012,0.0024)	(0.0245,0.0272)	(0.0082,0.0109)
	(e)	(f)	(g)	(h)
(r_1, r_2)	(0.0490,0.0531)	(0.0218,0.0245)	(0.1147,0.1530)	(0.0764,0.0792)

Theorem 2.1.

$$h(r) \geq C\left(\frac{r+n}{n}\right)^{1/q}$$

where $h(r) = \inf\{\text{ess. }\sup_{x\in\Omega} |u(x)|$: u is a nontrivial solution to (1.1) on $\Omega \subseteq B_n\}$, Ω is an open set with Lipschitz boundary and $C > 0$ is a constant independent of r.

Proof. If u is a nontrivial solution to (1.1) on Ω, we have

$$-\int_\Omega |\nabla u|^p dx + \int_\Omega |x|^r |u|^q dx = \int_\Omega (\Delta_p u + |x|^r |u|^{q-2} u) u\, dx = 0;$$

i.e.,

$$\int_\Omega |\nabla u|^p dx = \int_\Omega |x|^r |u|^q dx.$$

Then, by the hyperspherical coordinates,

$$
\begin{aligned}
\int_\Omega |x|^r |u|^q dx &= \int_{B_n} |x|^r |u_B|^q dx \\
&\leq (\text{ess. sup}_{x\in\Omega} |u(x)|)^q \\
&\quad \times \int_0^1 \rho^{r+n-1} d\rho \int_0^{2\pi} \int_{-\frac{\pi}{2}}^{\frac{\pi}{2}} \ldots \int_{-\frac{\pi}{2}}^{\frac{\pi}{2}} F(\phi, \theta_1, \ldots, \theta_{n-2}) d\phi d\theta_1 \ldots d\theta_{n-2} \\
&= (\text{ess. sup}_{x\in\Omega} |u(x)|)^q \frac{nV_n}{r+n};
\end{aligned}
$$

i.e.,

$$
\text{ess. sup}_{x\in\Omega} |u(x)| \geq \left(\frac{r+n}{nV_n}\right)^{1/q} \left(\int_\Omega |\nabla u|^p dx\right)^{1/q}, \tag{2.1}
$$

where $F(\phi, \theta_1, \ldots, \theta_{n-2}) = |det(J(\phi, \theta_1, \ldots, \theta_{n-2}))|$, $J(\phi, \theta_1, \ldots, \theta_{n-2})$ is the Jacobian matrix to the coordinate system transformation between the Cartesian coordinate system and the hyperspherical coordinate system, V_n is the volume of the unit ball B_n and

$$
u_B(x) = \begin{cases} u(x), & x \in \Omega, \\ 0, & x \notin \Omega. \end{cases}
$$

On the other hand, by the Sobolev imbedding theorem,

$$
\int_\Omega |\nabla u|^p dx = \int_\Omega |x|^r |u|^q dx \leq \int_\Omega |u|^q dx \leq c \left(\int_\Omega |\nabla u|^p dx\right)^{q/p},
$$

i.e.,

$$
\int_\Omega |\nabla u|^p dx \geq c^{p/(p-q)}, \tag{2.2}
$$

where $c > 0$ is a constant independent of r. Thus, from (2.1) and (2.2), for every nontrivial solution u to (1.1) on $\Omega \subseteq B_n$,

$$
\text{ess. sup}_{x\in\Omega} |u(x)| \geq \left(\frac{r+n}{nV_n}\right)^{1/q} c^{\frac{p}{q(p-q)}};
$$

i.e.,

$$
h(r) \geq C\left(\frac{r+n}{n}\right)^{1/q},
$$

where $C = c^{\frac{p}{q(p-q)}} V_n^{-\frac{1}{q}}$ is a constant independent of r.   □

Corollary 2.2.

$$
\lim_{r\to+\infty} \beta(r) = +\infty.
$$

where $\beta(r) = \{\text{ess. sup}_{x\in\Omega} |u(x)| \, | \, u$ is the ground state to (1.1) on an open set $\Omega \subseteq B_n$ with Lipschitz boundary.$\}$.

Remark 2.3. (1) From the above proof, it is clear that we have actually proved that the peak height of any nontrivial solution to p-Hénon equation (1.1) on an open set $\Omega \subseteq B_n$ with Lipschitz boundary goes to $+\infty$ as $r \to +\infty$.
(2) $\Omega = B_n$ is a special case.

2.2. **On a Square Domain in $\mathbb{R}^2$.** Consider the p-Hénon equation (1.1) on the hypercubic domain $\Omega = (-1, 1)^n$. Numerically, we set $n = 2$. If a solution of (1.1) is symmetric about the lines $x = 0$, $y = 0$ and $y = \pm x$, we say it is BN (Berestycki-Nirenberg) symmetric. Until now, theoretically, little is known about SBP and asymptotic behavior of its ground states. For numerical investigation, to maintain sufficient accuracy, over 10^6 square elements are used on $\Omega = (-1, 1)^2$ in our numerical computation. From many numerical results we obtained, we notice that the p-Hénon equation (1.1) on a square has much richer breaking phenomena than its counterpart on the unit disk due to the corner affect. First we notice that the positive BN symmetric solution always exists. On this solution, our numerical results for $r = 0$ have been presented in [9] and the contours of our numerical results for $r > 0$ are presented in (c) and (e) of Figs. 6-13. Due to the explicit dependence of the equation on x, SBP may occur. In this case, the positive BN symmetric solution gives up its ground state to some positive BN asymmetric solutions. It causes (1) SBP and (2) a peak breaking phenomenon (PBP), more specifically, when r increases and exceeds a certain value, the 1-peak BN symmetric positive solution becomes the 4-peak BN symmetric positive solution.

To investigate (1), SBP, we always use a BN asymmetric initial guess to start with the algorithm for capturing the ground state. If the numerically captured solution is BN symmetric, then our numerical experiment does not support SBP. In this case, we put the contours of BN symmetric numerical solutions in (a) of Figs. 6-13 as the contours of the ground states. Otherwise, the contours of BN asymmetric numerical solutions are presented in (b) and (d) of Figs. 6-13 as the contours of the ground states. The corresponding BN symmetric positive solution has higher energy level. Our minimax method is used to capture it. The contours of the BN symmetric numerical solutions are listed in (c) and (e) of Figs. 6-13. By our numerical results, we conclude that to the p-Hénon equation (1.1) on $(-1, 1)^2$, SBP always takes place when r increases and exceeds a certain value r_{b_1}. By (b) and (d), when SBP occurs, the BN asymmetric ground state is only symmetric about the line $y = x$ or $y = -x$ passing through the peak point. Generally, we would like to conjecture that to the p-Hénon equation (1.1) on the hypercubic domain $(-1, 1)^n$, SBP always occurs when r increases and exceeds a certain value r_{b_1}. In Table 6, we give information on the location of r_{b_1} from our numerical experiment. By (c) and (e), when r increases and exceeds a certain value r_{b_2}, the 1-peak BN symmetric positive solution in (c) becomes the 4-peak BN symmetric positive solution in (e), i.e., (2), PBP, takes place. In Table 7, we give information on the location of r_{b_2} from our numerical experiment.

Similar to the disk domain, more numerical experiments are carried out to investigate asymptotic behavior of the peak point and peak height of the positive ground state to (1.1) as $r \to +\infty$. For $(p, q) = (a)(1.75, 4.75)$, $(b)(1.75, 6.25)$, $(c)(2.0, 5.0)$, $(d)(2.0, 6.5)$, $(e)(2.5, 5.5)$, $(f)(2.5, 7.0)$, $(g)(3.0, 6.0)$, $(h)(3.0, 7.5)$, our numerical results on the peak points and peak heights are listed in Tables 4 and 5. From Table 4, it is quite natural to conclude that the peak point is of the form $(\alpha(r), \alpha(r))$ and $\alpha(r) \to 1$ as $r \to \infty$. Since the peak heights $\beta(r)$ listed in Table 5 are not monotone in r, we plot those $\beta(r)$ values in Fig. 14 from which one can see that for the ground states to the p-Hénon equation (1.1) on the square domain $(-1, 1)^2$, their peak heights, $\beta(r) \to 0$ as $r \to \infty$.
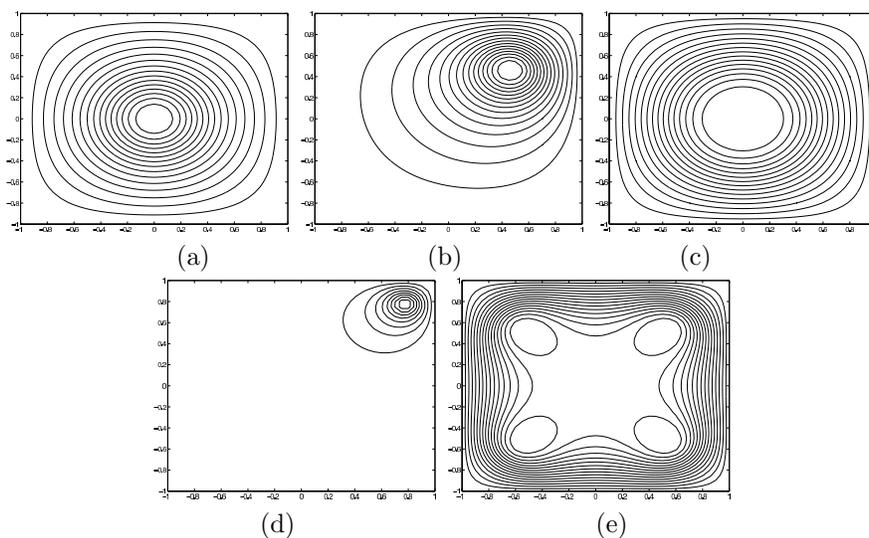
FIGURE 6. $p = 1.75$, $q = 4.75$: (a) $r = 0.01$; (b) $r = 1.0$, a ground state; (c) a 1-peak BN symmetric solution; (d) $r = 4.6$, a ground state; (e) a 4-peak BN symmetric solution
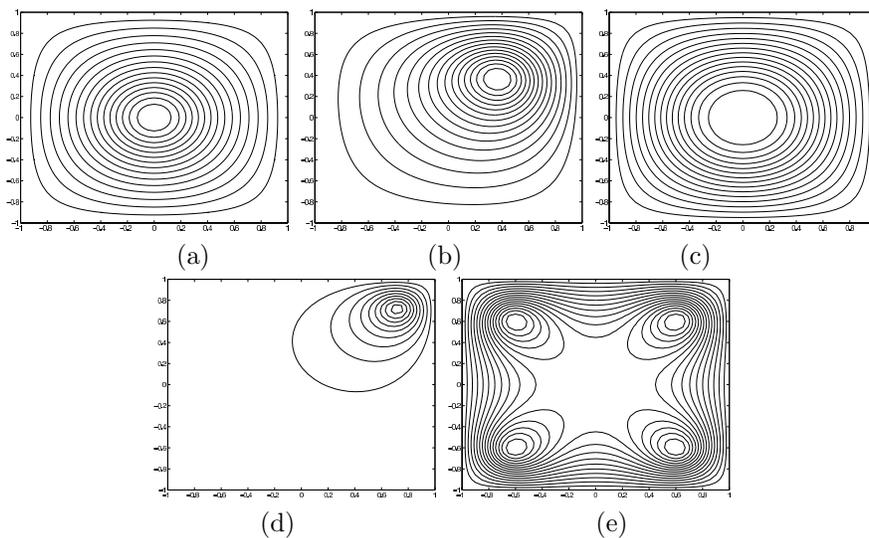

FIGURE 7. $p = 2.0$, $q = 5.0$: (a) $r = 0.01$; (b) $r = 1.0$, a ground state; (c) a 1-peak BN symmetric solution; (d) $r = 5.0$, a ground state; (e) a 4-peak BN symmetric solution
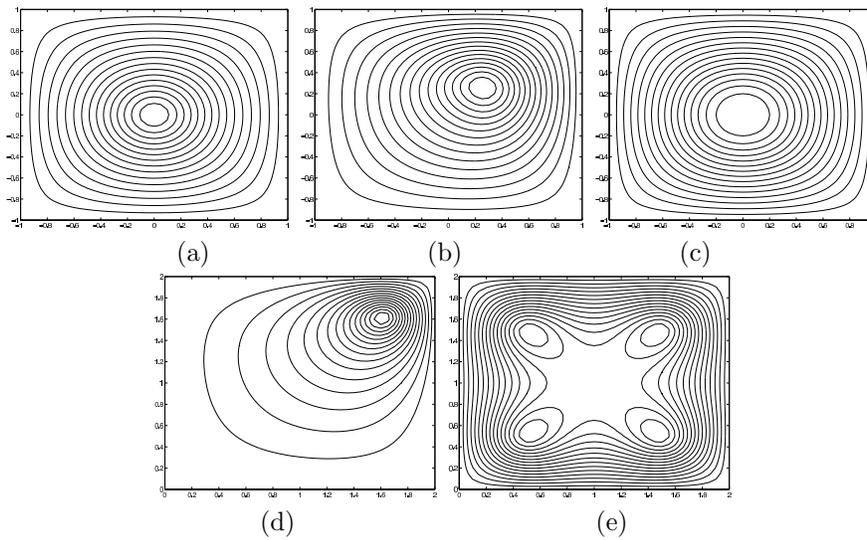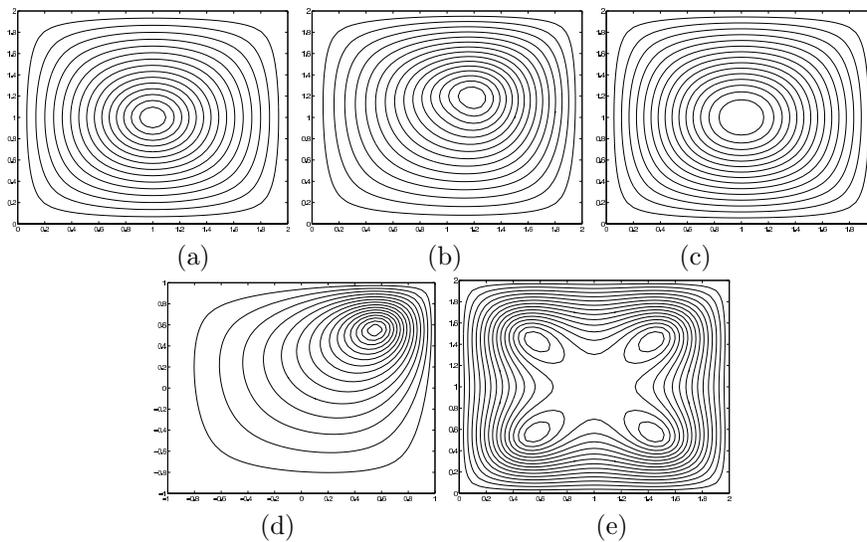
FIGURE 8. $p = 2.5$, $q = 5.5$: (a) $r = 0.01$; (b) $r = 1.0$, a ground state; (c) a 1-peak BN symmetric solution; (d) $r = 5.0$, a ground state; (e) a 4-peak BN symmetric solution

FIGURE 9. $p = 3.0$, $q = 6.0$: (a) $r = 0.01$; (b) $r = 1.0$, a ground state; (c) a 1-peak BN symmetric solution; (d) $r = 5.3$, a ground state; (e) a 4-peak BN symmetric solution
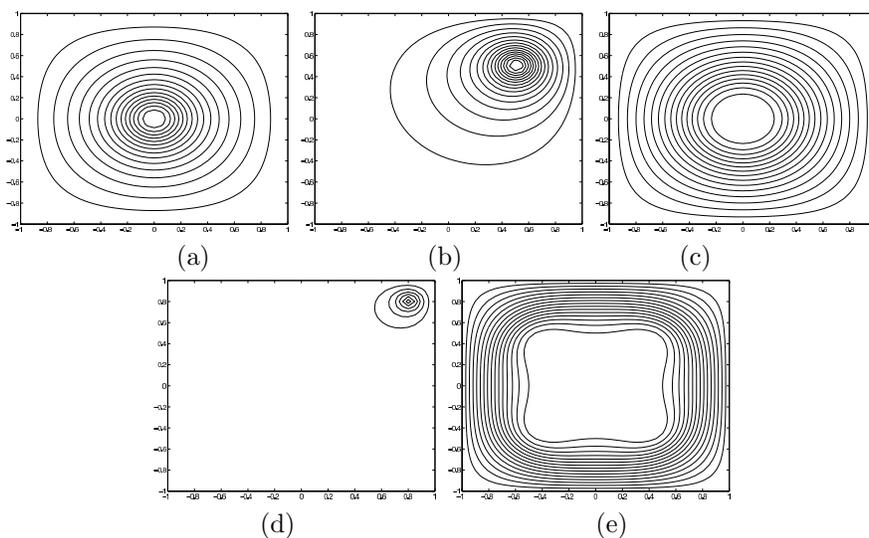
FIGURE 10. $p = 1.75$, $q = 6.25$: (a) $r = 0.01$; (b) $r = 1.0$, a ground state; (c) a 1-peak BN symmetric solution; (d) $r = 4.6$, a ground state; (e) a 4-peak BN symmetric solution
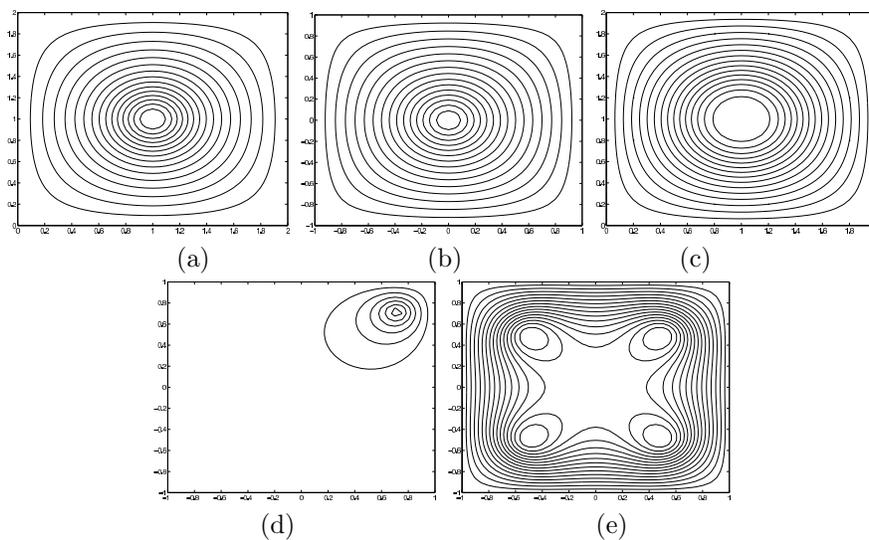

FIGURE 11. $p = 2.0$, $q = 6.5$: (a) $r = 0.01$; (b) $r = 1.0$, a ground state; (c) a 1-peak BN symmetric solution; (d) $r = 5.0$, a ground state; (e) a 4-peak BN symmetric solution

FIGURE 12. $p = 2.5$, $q = 7.0$: (a) $r = 0.01$; (b) $r = 1.0$, a ground state; (c) a 1-peak BN symmetric solution; (d) $r = 5.0$, a ground state; (e) a 4-peak BN symmetric solution
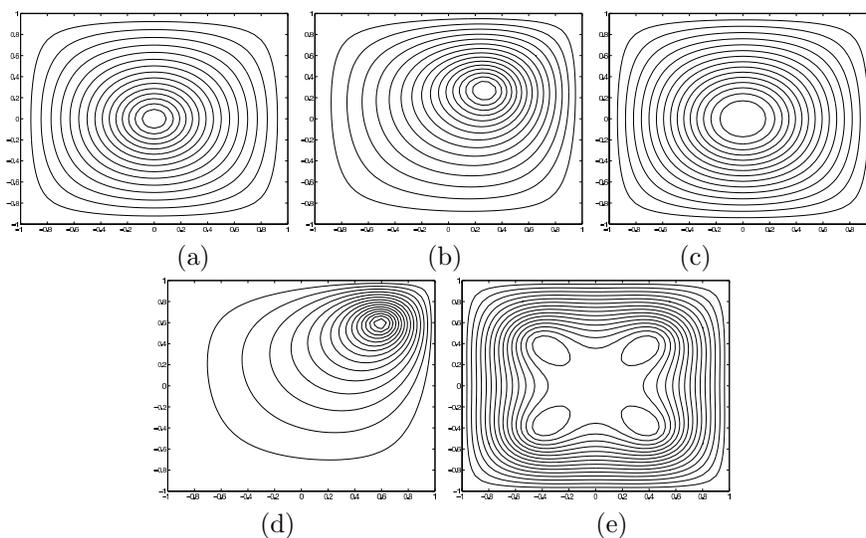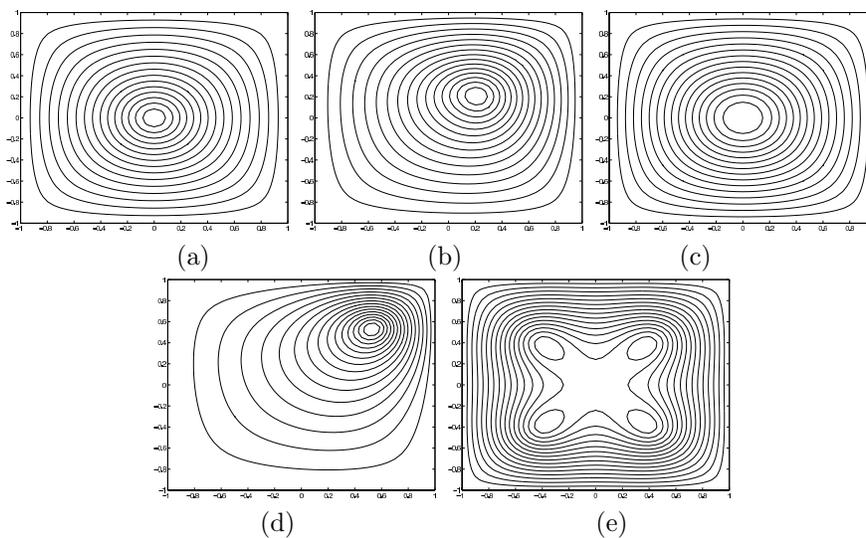

FIGURE 13. $p = 3.0$, $q = 7.5$: (a) $r = 0.01$; (b) $r = 1.0$, a ground state; (c) a 1-peak BN symmetric solution; (d) $r = 5.3$, a ground state; (e) a 4-peak BN symmetric solution

TABLE 4. Values for α in Equation (1.1) with (α, α) as peak point of its ground state and (p, q): (a) (1.75,4.75), (b) (1.75,6.25), (c) (2.0,5.0), (d) (2.0,6.5), (e) (2.5,5.5), (f) (2.5,7.0), (g) (3.0,6.0), (h) (3.0,7.5)

r	(a)	(b)	(c)	(d)	(e)	(f)	(g)	(h)
1	0.473	0.486	0.374	0.386	0.259	0.273	0.190	0.210
10	0.887	0.905	0.833	0.831	0.758	0.743	0.700	0.679
20	0.938	0.951	0.909	0.908	0.862	0.852	0.824	0.809
30	0.958	0.967	0.936	0.937	0.903	0.896	0.876	0.865
40	0.965	0.975	0.952	0.952	0.926	0.919	0.914	0.895
50	0.971	0.982	0.961	0.961	0.940	0.935	0.922	0.914
60	0.976	0.987	0.967	0.967	0.950	0.945	0.934	0.927
70	0.982	0.991	0.972	0.972	0.957	0.952	0.943	0.937
80	0.984	0.993	0.975	0.974	0.962	0.958	0.950	0.944

TABLE 5. Values for β in Equation (1.1) with β as peak height of its ground state and (p, q): (a) (1.75,4.75), (b) (1.75,6.25), (c) (2.0,5.0), (d) (2.0,6.5), (e) (2.5,5.5), (f) (2.5,7.0), (g) (3.0,6.0), (h) (3.0,7.5)

r	(a)	(b)	(c)	(d)	(e)	(f)	(g)	(h)
1	3.6277	2.8676	3.6791	2.7576	3.9439	2.8144	4.2204	2.9194
10	3.6149	2.9320	4.0596	2.9330	5.4975	3.5136	7.3453	4.2542
20	1.6608	1.7568	1.9677	1.8104	2.9495	2.3255	4.3500	3.0147
30	0.6560	0.9509	0.8034	0.9964	1.2828	1.3361	2.0116	1.8052
40	0.2510	0.4869	0.3050	0.5269	0.5091	0.7234	0.8359	1.0066
50	0.0861	0.2421	0.1111	0.2666	0.1920	0.3773	0.3269	0.5392
60	0.0301	0.1250	0.0395	0.1338	0.0704	0.1929	0.1230	0.2807
70	0.0105	0.0659	0.0138	0.0663	0.0252	0.0972	0.0451	0.1441
80	0.0036	0.0348	0.0048	0.0325	0.0089	0.0485	0.0162	0.0728

TABLE 6. $r_{b_1} \in (r_1, r_2)$ for (p, q): (a) (1.75,4.75), (b) (1.75,6.25), (c) (2.0,5.0), (d) (2.0,6.5), (e) (2.5,5.5), (f) (2.5,7.0), (g) (3.0,6.0), (h) (3.0,7.5)

	(a)	(b)	(c)	(d)
(r_1, r_2)	(0.1055,0.1094)	(0.0313,0.0352)	(0.1406,0.1445)	(0.1012,0.1058)
	(e)	(f)	(g)	(h)
(r_1, r_2)	(0.3006,0.3046)	(0.1367,0.1406)	(0.4572,0.461)	(0.2376,0.2411)

TABLE 7. $r_{b_2} \in (r_1, r_2)$ for $(p, q) = (a)(1.75, 4.75)$, $(b)(1.75, 6.25)$, $(c)(2.0, 5.0)$, $(d)(2.0, 6.5)$, $(e)(2.5, 5.5)$, $(f)(2.5, 7.0)$, $(g)(3.0, 6.0)$, $(h)(3.0, 7.5)$

	(a)	(b)	(c)	(d)
(r_1, r_2)	(1.7461,1.75)	(2.2461,2.25)	(1.7695,1.7734)	(3.3789,3.3828)
	(e)	(f)	(g)	(h)
(r_1, r_2)	(3.3867,3.3906)	(3.707,3.7109)	(3.4375,3.4399)	(3.8125,3.8164)

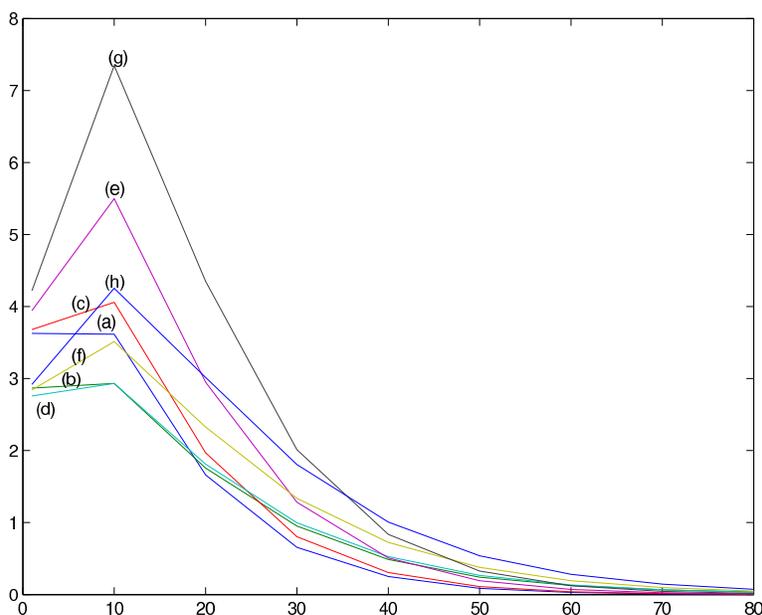FIGURE 14. $\beta(r)$ curves for (p, q): (a) (1.75,4.75), (b) (1.75,6.25), (c) (2.0,5.0), (d) (2.0,6.5), (e)(2.5,5.5), (f) (2.5,7.0), (g) (3.0,6.0), (h) (3.0,7.5) in r-β coordinate system. All $\beta(r)$ curves approach zero as $r \to +\infty$

Theorem 2.4. *Assume the bounded open domain $\Omega \subset \mathbb{R}^n$ satisfies $max_{x \in \Omega}|x| > 1$ where $|x| = (\sum_{k=1}^n x_k^2)^{\frac{1}{2}}$ and $r > 0$, $1 < p < q < p^*$ in (1.1). If u_r^* is a ground state of (1.1), then $u_r^* \to 0$ as $r \to \infty$.*

Proof. We have

$$J(u) = \int_\Omega \left[\frac{1}{p} |\nabla u(x)|^p - \frac{|x|^r}{q} |u(x)|^q \right] dx. \tag{2.3}$$

First by our minimax characterization of solutions in [9], for each fixed $r > 0$ and each $v_r \in W_0^{1,p}(\Omega)$ with $\|v_r\| = \int_\Omega |\nabla v_r(x)|^p dx = 1$, $p(v_r) = t_r v_r$ where $t_r = \arg \frac{d}{dt} J(tv_r) = 0$ or

$$t_r = \left(\int_\Omega |x|^r |v_r(x)|^q dx \right)^{\frac{1}{p-q}}. \tag{2.4}$$

Since we have $\hat{u}_r = p(\hat{v}_r) = \hat{t}_r\hat{v}_r$ for every nontrivial solution $\hat{u}_r$ of (1.1) where $\hat{v}_r(x) = \frac{\hat{u}_r(x)}{\|\hat{u}_r\|}$ and

$$\hat{t}_r = \|\hat{u}_r\| = \left(\int_\Omega |x|^r |\hat{v}_r(x)|^q dx\right)^{\frac{1}{p-q}},$$

a ground state is of the form $u_r^* = p(v_r^*)$ where

$$v_r^* = \arg \min_{v_r \in W_0^{1,p}(\Omega), \|v_r\|=1} J(p(v_r)). \tag{2.5}$$

By plugging t_r in (2.4) into $J(t_r v_r)$ in (2.3), we obtain

$$J(t_r v_r) = \frac{t_r^p}{p} - \frac{t_r^q}{q}\int_\Omega |x|^r |v_r(x)|^q \, dx = t_r^p\left(\frac{1}{p} - \frac{1}{q}\right)$$
$$= \left[\int_\Omega |x|^r |v_r(x)|^q \, dx\right]^{p/(p-q)} \left(\frac{1}{p} - \frac{1}{q}\right). \tag{2.6}$$

Thus $u_r^* = p(v_r^*) = t_r^* v_r^*$ where $v_r^* \in W_0^{1,p}(\Omega)$ with $\|v_r^*\| = 1$ and

$$t_r^{*(p-q)} = \int_\Omega |x|^r |v_r^*(x)|^q dx. \tag{2.7}$$

Since the bounded open domain Ω satisfies $\max_{x \in \Omega}|x| > 1$, there exists $\bar{x} \in \Omega$ such that the ball of center at $\bar{x} = (\bar{x}_1, \ldots, \bar{x}_n)$ and radius $\bar{r} > 0$, $B(\bar{x}, \bar{r}) \subset \Omega \setminus B_n$. Let

$$\bar{v}(x) = \begin{cases} (\bar{r}^2 - \sum_{k=1}^n (x_k - \bar{x}_k)^2)^2, & x = (x_1, \ldots, x_n) \in B(\bar{x}, \bar{r}), \\ 0, & x = (x_1, \ldots, x_n) \in \Omega \setminus B(\bar{x}, \bar{r}). \end{cases}$$

Denote

$$I(r) = \int_{\Omega \setminus B_n} |x|^r c_0^q |\bar{v}(x)|^q dx \to +\infty \quad \text{as } r \to +\infty,$$

where $c_0 = \|\bar{v}\|^{-1}$. By (2.5) for each fixed $r > 0$, we have

$$J(t_r^* v_r^*) = \left[\int_\Omega |x|^r |v_r^*(x)|^q \, dx\right]^{p/(p-q)} \left(\frac{1}{p} - \frac{1}{q}\right) \le J(p(v))$$
$$= \left[\int_\Omega |x|^r |v(x)|^q \, dx\right]^{p/(p-q)} \left(\frac{1}{p} - \frac{1}{q}\right)$$

for any $v \in W_0^{1,p}(\Omega)$ with $\|v\| = 1$. In particular, if we note $1 < p < q$, we have

$$J(t_r^* v_r^*) = t_r^{*p}\left(\frac{1}{p} - \frac{1}{q}\right)$$
$$\le \left[\int_\Omega |x|^r c_0^q |\bar{v}(x)|^q dx\right]^{p/(p-q)} \left(\frac{1}{p} - \frac{1}{q}\right) \le I(r)^{p/(p-q)}\left(\frac{1}{p} - \frac{1}{q}\right) \to 0.$$

Thus $t_r^* \to 0$; i.e., $u_r^* = t_r^* v_r^* \to 0$ as $r \to +\infty$ since $\|v_r^*\| = 1$. $\qquad\square$

Remark 2.5. *(1) By Remark 2.3, to the peak height $\beta_a(r)$ of the ground states of (1.1) on $\Omega = (-a, a)^n$, $a \le \frac{1}{\sqrt{n}}$, we have*

$$\lim_{r \to \infty} \beta_a(r) = +\infty.$$

(2) To the ground states $u_a(r)$ of (1.1) on $\Omega = (-a, a)^n$, $a > \frac{1}{\sqrt{n}}$, we have

$$\lim_{r \to \infty} u_a(r) = 0.$$

$\Omega = (-1, 1)^n$ *is a special case.*

(3) The conclusion $u(r) \to 0$ in the theorem is a little different from $\beta(r) \to 0$ suggested by Table 4. On any bounded open domain $\Omega \subset \mathbb{R}^n$ with $max_{x\in\Omega}|x| = (\sum_{k=1}^{n} x_k^2)^{\frac{1}{2}} > 1$, we would like to conjecture

$$\beta(r) \to 0,$$

where $\beta(r)$ is the peak height of the ground states of (1.1).

2.3. More on 1-peak BN asymmetric positive solutions.

In the last subsection, our numerical results suggest that to the p-Hénon equation (1.1) on the square domain $\Omega = (-1,1)^2$, when SBP occurs, the BN asymmetric ground states are only symmetric about the line $y = x$ or $y = -x$ passing through the peak point. Then, it is interesting to ask if there exist 1-peak BN asymmetric positive solutions which are symmetric about $x = 0$ or $y = 0$.

Such a solution was numerically captured first by accident then on purpose by enforcing an even-symmetry about the x-axis. By the symmetry of the p-Hénon equation on the square, it is clear that there are actually four such solutions. According to our numerical computation, such a solution has higher energy than the ground state. So they are more unstable than the ground states. In Figs. 15-18, the contours of numerical results for such solutions are listed in the second row; the contours of numerical results for ground states are displayed in the first row; corresponding solution energies J and p, q, r values are given in the captions.

We also did numerical experiments to investigate (1.1) on $\Omega = (-1,1)$, a two-point boundary value problem. The profiles of these numerical results are presented in the third row of Figs. 15-18 with associated p, q, r values in the captions.
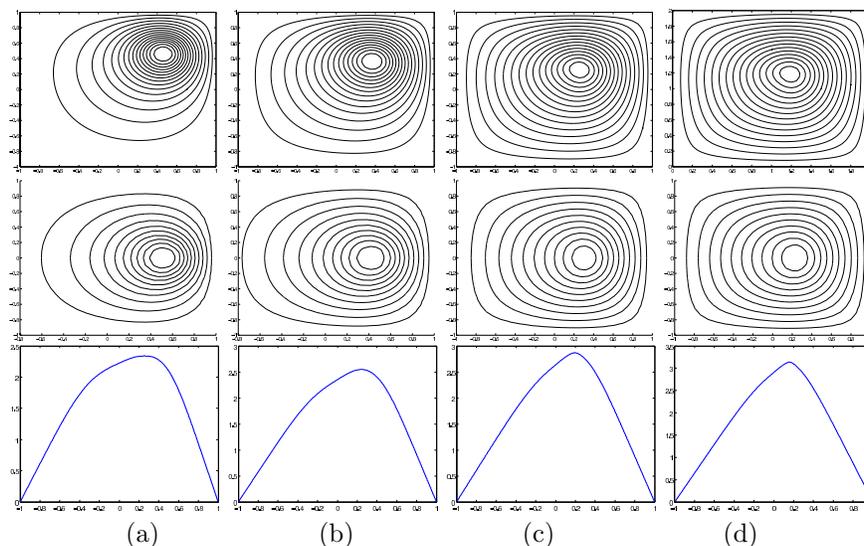

(a)   (b)   (c)   (d)

FIGURE 15. $r = 1.0$: (a) $p = 1.75$, $q = 3.75$, $J = 9.30, 9.92$; (b) $p = 2.0$, $q = 4.0$, $J = 12.31, 12.84$; (c) $p = 2.5$, $q = 4.5$, $J = 21.70, 22.10$; (d) $p = 3.0$, $q = 5.0$, $J = 40.38, 40.71$
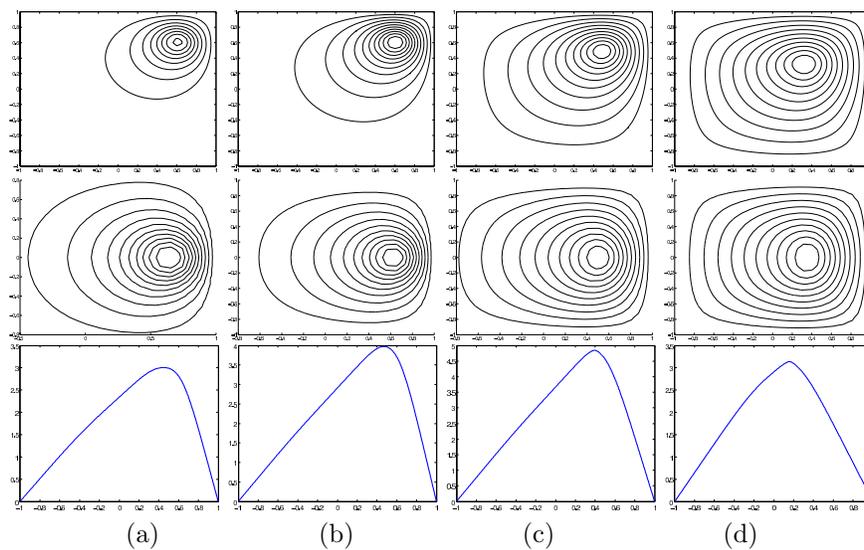
FIGURE 16.   (a) $p = 1.75$, $q = 3.75$, $r = 2.0$, $J = 10.91, 13.47$; (b)
$p = 2.0$, $q = 4.0$, $r = 3.0$, $J = 19.44, 27.40$; (c) $p = 2.5$, $q = 4.5$,
$r = 3.0$, $J = 54.97, 73.31$; (d) $p = 3.0$, $q = 5.0$, $r = 2.0$, $J = 94.63, 103.86$
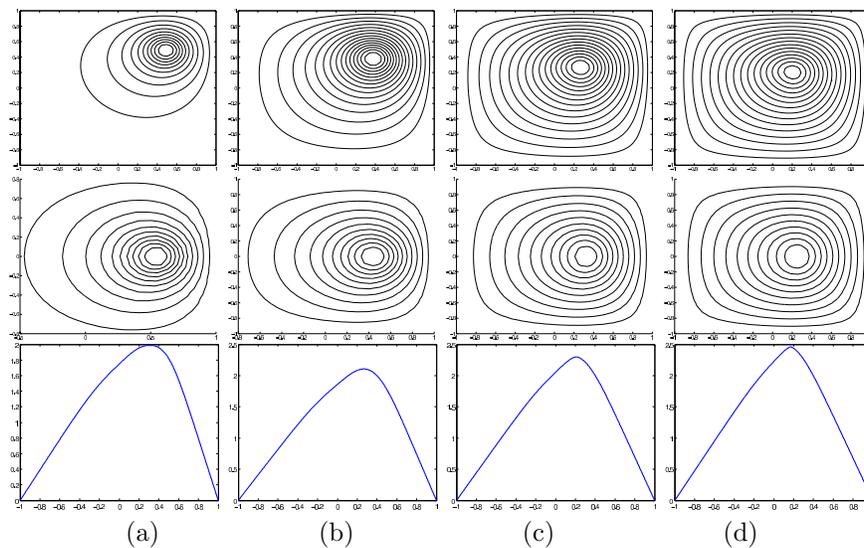

FIGURE 17. $r = 1.0$: (a) $p = 1.75$, $q = 4.75$, $J = 6.25, 6.62$;
(b) $p = 2.0$, $q = 5.0$, $J = 7.84, 8.16$; (c) $p = 2.5$, $q = 5.5$, $J = 11.88, 12.15$; (d) $p = 3.0$, $q = 6.0$, $J = 18.61, 18.86$
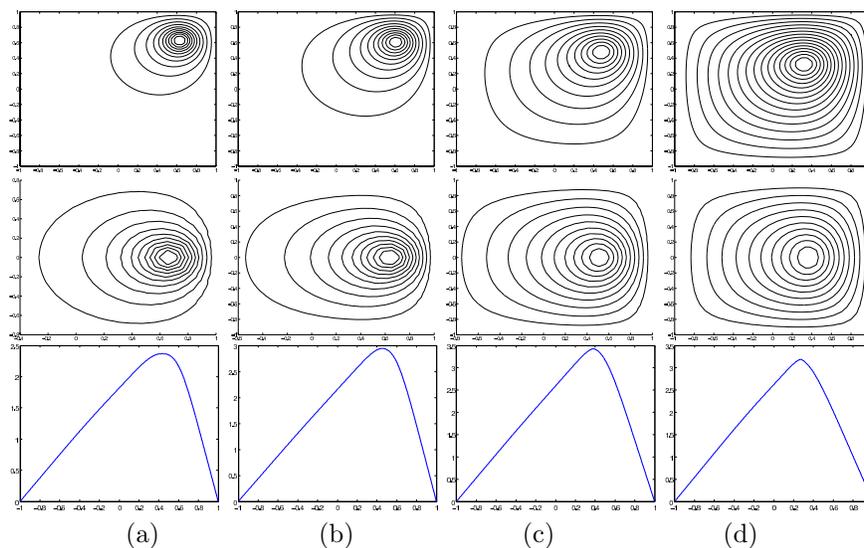
FIGURE 18. (a) $p = 1.75$, $q = 4.75$, $r = 2.0$, $J = 6.91, 8.21$; (b) $p = 2.0$, $q = 5.0$, $r = 3.0$, $J = 11.01, 14.43$; (c) $p = 2.5$, $q = 5.5$, $r = 3.0$, $J = 24.48, 30.96$; (d) $p = 3.0$, $q = 6.0$, $r = 2.0$, $J = 35.85, 39.17$

3. Conclusions and Conjectures

Many numerical experiments are carried out for 1-peak positive solutions to the p-Hénon equation (1.1) on the unit disk B_2 and the square $\Omega_2 = (-1, 1)^2$. From our numerical results and Theorem 2.1, for fixed $1 < p < q < p^*$, we have the following conclusions.

Conclusion I. As a bifurcation phenomenon, SBP always occurs when r increases and exceeds a certain value, on both B_2 and Ω_2. When SBP takes place, the ground states are 1-peak solutions on B_2 and 1-peak solutions with peak point (a_1, a_2), where $|a_1| = |a_2| > 0$, on Ω_2.

Conclusion II. On B_2, the peak point of the ground state goes to the boundary of B_2 and its peak height tends to $+\infty$ as $r \to +\infty$. On the other hand, the top of the 1-peak radially symmetric solution becomes flatter as r increases and its peak height tends to $+\infty$ as $r \to +\infty$.

Conclusion III. On Ω_2, when SBP occurs, 1-peak BN asymmetric ground state is only symmetric about the line $y = x$ or $y = -x$ passing through its peak point. The peak point of the ground state goes to a corner of Ω_2 and its peak height tends to 0 as $r \to +\infty$. When r increases and exceeds a certain value, PBP takes place, i.e., the 1-peak BN symmetric solution becomes a 4-peak BN symmetric solution. Clearly PBP is not a bifurcation phenomenon since the old solution is only replaced by a new solution.

Conclusion IV. On Ω_2, when r increased, there is 1-peak, BN asymmetric, non-ground state, positive solution with its peak point $(x_p, 0)$, $x_p > 0$ or $(0, y_p)$, $y_p > 0$ which is symmetric about the line $y = 0$ or $x = 0$.

Based on our numerical results which are still unique in the literature, Theorem 2.1 and Theorem 2.4, for each fixed $1 < p < q < p^*$, we have the following conclusions and conjectures for the p-Hénon equation (1.1) in $\mathbb{R}^n$. On the hypercubic domain $\Omega_n = (-1, 1)^n$, if Ω_n is symmetric about a hyperplane passing through the origin, then a solution is also symmetric about it. We say such a solution is a BN symmetric solution.

Conclusion I. On any bounded open set $\Omega \subseteq B_n$ with Lipschitz boundary, the peak height of the solutions is proved in Theorem 2.1 to tend to $+\infty$ as $r \to +\infty$.

Conclusion II. On any bounded open domain $\Omega \subset \mathbb{R}^n$ with

$$\max_{x \in \Omega} |x| = (\sum_{k=1}^n x_k^2)^{\frac{1}{2}} > 1,$$

the ground states, as proved in Theorem 2.4 , tend to 0 as $r \to +\infty$.

Conjecture I. On the unit ball B_n, the top of the radial positive solution becomes flatter as r increases. As a bifurcation of the 1-peak radial solution in r, a 1-peak non-radial positive ground state solution exists, i.e., SBP occurs, when r increases and exceeds a certain value. Its peak point goes to the boundary.

Conjecture II. On the hypercube $\Omega_n = (-1, 1)^n$, as a bifurcation of the BN symmetric positive solution in r, a 1-peak BN asymmetric positive ground state solution exists, i.e., SBP occurs, when r increases and exceeds a certain value. The peak point of the ground state is $(a_1, \ldots, a_n)$, where $a_i = a$ or $-a$, $i = 1, \ldots, n$ and $0 < a < 1$ is some number. If Ω_n is symmetric about a hyperplane passing through the origin and the peak point, the ground state keeps this symmetry and if Ω_n is symmetric about a hyperplane only passing through the origin, the ground state loses this symmetry. The peak point of the ground state goes to a vertex of Ω_n.

Conjecture III. On any open bounded domain $\Omega \subset \mathbb{R}^n$ with $max_{x \in \Omega} |x| = (\sum_{k=1}^n x_k^2)^{\frac{1}{2}} > 1$, the peak height of the ground states goes to 0 as $r \to +\infty$.

Conjecture IV. On the hypercube $\Omega_n = (-1, 1)^n$, when r increases and exceeds a certain value, the peak of the 1-peak BN symmetric positive solution breaks into 2n peaks and when r increases, 1-peak positive solutions with their peak points $(x_1, \ldots, x_n)$ satisfying one of the followings, (**1**) $x_1 = \cdots = x_n > 0$, (**2**) $x_1 = \cdots = x_{n-1} > 0, x_n = 0, \ldots$, (**n**) $x_1 > 0, x_2 = \cdots = x_n = 0$, will show up.

We hope that our numerical evidences can stimulate further analytic verifications of those new phenomena.

References

[1] H. Brezis; *Symmetry in Nonlinear PDE's*, Proceedings of Symposia in Pure Mathematics (American Mathematical Society, Providence, Rhode Island) (M.Giaquinta, J.Shatah and S.R.S.Varadham ed.), Vol. 65, 1996, pp. 1-12.

[2] J. Byeon and Z. Q. Wang; *On the Henon equation: asymptotic profile of ground states. I*, Ann. Inst. H. Poincar Anal. Non Linaire 23(2006), no. 6, 803–828.

[3] J. Byeon and Z. Q. Wang; *On the Henon equation: asymptotic profile of ground states. II*, J. Differential Equations 216(2005), no. 1, 78–108.

[4] G. Chen, W.-M. Ni and J. Zhou; *Algorithms and visualization for solutions of nonlinear elliptic equations*, Internat. J. Bifur. Chaos 10(2000) 1565-1612.

[5] J. I. Diaz; *Nonlinear Partial Differential Equations and Free Boundaries*, Vol. I, Elliptic Equations, Research Notes in Mathematics 106, Pitman Publishing, Boston, 1985.

[6] M. Henon; Numerical experiments on the stability of spherical stellar systems, Astronomy and Astrophysics, 24 (1973), 229–238.

[7] D. Smets and M. Willem; *Partial symmetry and asymptotic behavior for some elliptic variational problems*, Calc. Var., 18(2003), 57-75.

[8] D. Smets, M. Willem and J. Su; *Non-radial ground states for the Henon equation*, Commun. Contemp. Math., 4(2002), no. 3, 467-480.

[9] X. Yao and J. Zhou; *A minimax method for finding multiple critical points in Banach spaces and its application to quasi-linear elliptic PDE*, SIAM J. Sci. Comp., 26(2005), 1796-1890.

[10] X. Yao and J. Zhou; *Unified convergence results on a minimax algorithm for finding multiple critical points in Banach spaces*, SIAM J. Num. Anal., 45(2007), 1330-1347.

[11] X. Yao and J. Zhou; *Numerical methods for computing nonlinear eigenpairs. Part I. Isohomogenous cases.*, SIAM J. Sci. Comp., 29(2007), 1355-1374.

XUDONG YAO

DEPARTMENT OF MATHEMATICS, SHANGHAI NORMAL UNIVERSITY, SHANGHAI, 200234, CHINA
    E-mail address: xdyao@shnu.edu.cn

JIANXIN ZHOU

DEPARTMENT OF MATHEMATICS, TEXAS A&M UNIVERSITY, COLLEGE STATION, TX 77843, USA
    E-mail address: jzhou@math.tamu.edu